A METHOD FOR DETERMINING THE CTOD AT CRACKING INITIATION - APPLICATION TO THE CHARACTERIZATION OF THE FRACTURE TOUGHNESS OF COPPER

T. Pardoen

Université catholique de Louvain, Département des Sciences des Matériaux et Procédés, PCIM, Bâtiment Réaumur, 2 Place Sainte Barbe, B-1348 Louvain-la-Neuve, Belgium
e-mail : pardoen@pcim.ucl.ac.be

ABSTRACT

A method is proposed for measuring the Crack Tip Opening Displacement (CTOD) at physical cracking initiation in ductile materials. The method requires a few precracked specimens to be loaded at different levels in order to involve various crack extensions. The total opening of the blunted precrack, δ_1, the opening of the tearing crack, δ_2, and the ductile tearing extension are measured for each specimen. The unloaded CTOD at cracking initiation is equal to the difference δ_1 - δ_2 extrapolated to zero crack extension. Simple fracture mechanics arguments are used to model the reverse plasticity during unloading. The potential of the method is illustrated by a brief discussion of results obtained on cracked copper specimen. That study was devoted to the analysis of the effect of the loading configuration on the cracking initiation toughness.

INTRODUCTION

The detection of cracking initiation is a remnant difficulty in fracture testing of ductile materials. Resistance curve methods, like the J_R curve method (ASTM [1], ESIS [2]), circumvent the problem by defining engineering fracture toughness parameters. Although engineering fracture toughness measures sometimes differs very much from the fracture toughness at physical cracking initiation, engineering values are adequate in many instances of material properties characterization or structural integrity assessments. For instance, when the objective is only to compare the fracture toughness of similar materials, the J_R curve method is most often adequate. Furthermore, in some very tough metals or in adhesive joints, the main issue is not cracking initiation but rather crack propagation, or sometimes solely the steady-state toughness. However, only the fracture toughness at cracking initiation (K_{Ic} or K_c, G_{Ic} or G_c, J_{Ic} or J_c) is directly connected to the "intrinsic" work per unit area spent in the fracture process zone. Indeed, during crack propagation, "extrinsic" effects related to the plastic wake and non-proportional loading in the active plastic zone (and other possible constraint effects) render very intricate the link with the micromechanisms of damage and cracking [3]. Also, in some applications, a more accurate estimate of the true fracture toughness is necessary because more precision is required or because the J_R curve technique is found too sensitive to the definition of the offset of the blunting line (e.g. Li and Bakker [4]).

The analysis of the load-displacement curve does usually not allow detection of fracture initiation in ductile materials. Several indirect methods can be used in order to detect cracking initiation (e.g. potential drop technique, acoustic emissions, and resonance frequency), whose success varies from material to material and from geometry to geometry. Furthermore, all these methods rely on a preliminary assessment of their sensibility by a comparison to an independent, accurate detection of cracking initiation. Theoretically, a stretch zone width measurement can be correlated to the value of the CTOD at cracking initiation. Stretch zone width measurement requires only one broken specimen and does not necessitate the detection of cracking initiation. However, this method gives large experimental scatter, which depends on the way the measurement is performed (see Pluvinage and Lanvin [5]). When time is not a primary limitation, the most pertinent way to evaluate fracture toughness at cracking initiation in ductile material remains the metallographical observation of the crack tip in unloaded specimens (see also Ebrahimi and Seo [6]). In addition, this procedure gives insight into the micromechanisms of damage in front of the crack tip. Usually, one serious complication of such method is that the test must be precisely interrupted at cracking initiation, a condition that can necessitate many experimental attempts. This difficulty is addressed in the first section of the paper by suggesting a new simple method which allows to determine the critical CTOD without requiring to interrupt the test at cracking initiation (see also [7] for more details).

Unless the test is made in-situ in the microscope (giving then only a surface information), metallographical observation requires unloading of the specimen (allowing bulk analysis by grinding and polishing of the specimens). During unloading, the crack partially closes as a result of reverse plastic yielding, a phenomenon which has been studied in much details in the "fatigue community" (Rice [8]) but which is generally not addressed in works involving metallographical observation of monotonically loaded cracked specimen. When fracture testing of ductile materials are performed under large scale yielding (LSY) conditions, the extension of reverse plasticity during unloading is small in comparison to the extension of plasticity during loading. Reverse plasticity then remains limited to the small-scale range and the plastic stretching of the crack face due to reverse plasticity remains a tiny fraction of the crack opening during loading. However, when small-scale yielding (SSY) conditions dominate during loading, reverse plasticity may, in low strain hardening materials, cause a decrease of the CTOD by about half its value under load [8].[1] This problem of reverse plasticity during unloading is addressed in the second section of this paper where a simple model based on fracture mechanics arguments is discussed.

This method has been used in an application in which precise values of fracture toughness at cracking initiation were requested, namely an analysis of constraint effects at cracking initiation in copper specimens through a comparison between Circumferentially Cracked Round Bars (CRB) and Single Edge Notched Beam Specimens (SENB) (Pardoen *et al.* [10]). The main results of that investigation are briefly described in the third section for the sake of illustrating the method.

PRESENTATION OF THE METHOD

Fig. 1a shows a sketch of the evolution of the crack tip profile as a function of the loading, starting from the precracked, unloaded state to a situation with significant amount of ductile tearing. Cracking initiates between steps 3 and 4, which only differ by a slight increase of the remote loading. Crack extension is made of two parts: crack growth due to blunting, Δa_{bl}, and crack extension corresponding to the real ductile tearing, Δa_{tear} (as depicted on Fig. 1a, step 6). The "unloaded CTOD at cracking initiation", δ^*_c, can be estimated from the difference between δ_1 and δ_2, where δ_1 is the total opening of the blunted crack and δ_2 is the opening of the tearing crack at the blunted crack tip (Fig. 1a, step 6). Fig. 1b shows how δ^*_c is obtained as the value of $\delta_1 - \delta_2$ when Δa_{tear} tends toward 0. Several effects cause the difference $\delta_1 - \delta_2$ to diverge from δ^*_c when Δa_{tear} increases: plastic rotation; large strain effects; variation of the unloading behavior as a function of the amount of ductile tearing (especially, the extending crack tip may completely close before total unloading, which can prevent further closing of the crack mouths).

The method requires loading of a few precracked specimens in such a way as to obtain various crack lengths (as in the multiple-specimen J_R curve methodology). After unloading, the specimens are machined, embedded in an edge-retention resin, ground and polished. Polished specimens are observed using an optical microscope and the parameters δ_1, δ_2 and Δa_{tear} are measured on micrographs. Each specimen is ground and polished several times in order to allow measurement of $\delta_1 - \delta_2$ and Δa_{tear} at various locations along the crack front. In the CRB specimens, a elementary trigonometric correction was applied in order to calculate the real crack advances from the projected values. Each specimen can thus be characterized by average values of $\delta_1 - \delta_2$ and Δa_{tear}. A too large crack extension, typically larger than 2 mm, must be avoided because of the increasing error on $\delta_1 - \delta_2$ (difference of two large values). Too small crack extensions, typically smaller than 25 μm, bring about large uncertainties in the measurement of Δa_{tear}. For specimens presenting crack tunneling (i.e. larger crack extensions in the some regions of the specimen due to a higher constraint), it is important to perform measurements at the surface and at the center of the specimen in order to get a good estimate of the average crack growth. A major advantage of this method is that it does not imply that the

[1] During crack propagation, the CTOD at the advancing crack tip can decrease by more than 50% due to residual strains in the crack wake and to non-proportional loading in the active plastic zone (Budiansky and Hutchinson [9]). These effects can involve contact of the crack faces.

specimens be unloaded exactly at cracking initiation, which may require many trials and errors. This method also avoids the problem of deciding whether or not the occurrence of small shear microcracks at the crack tip (like those observed in Ref. [6]) should be considered as the initiation of cracking.

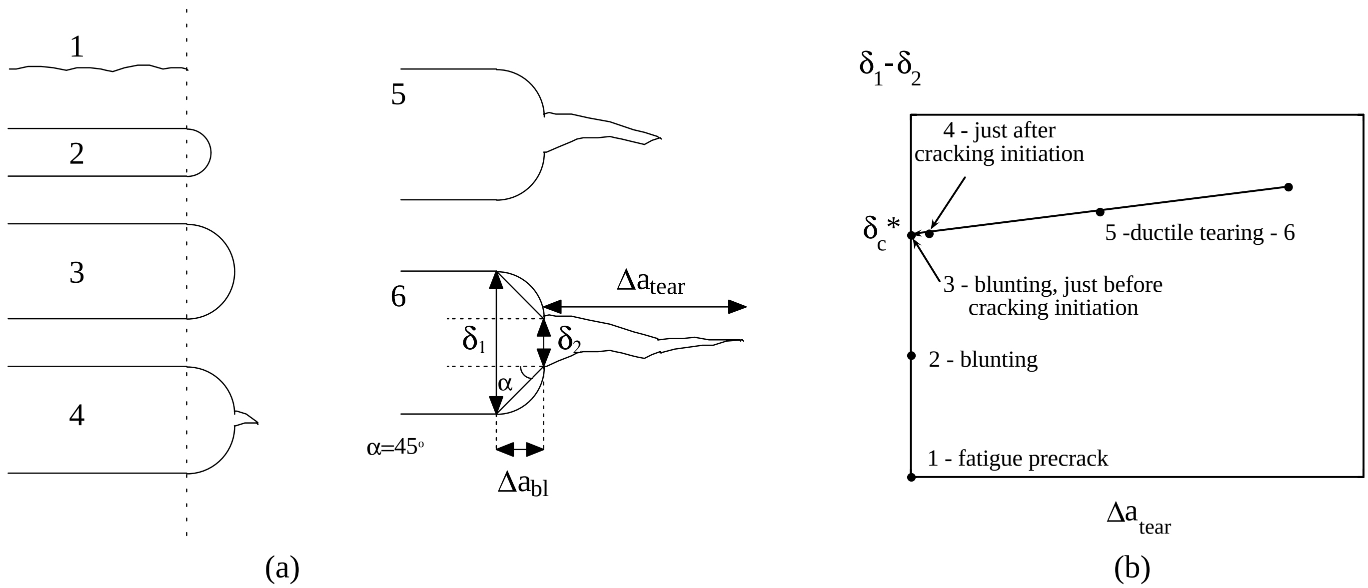

Figure 1. (a) Sketch of the evolution of the crack tip profile and definition of the crack openings δ_1 - δ_2 and crack extensions Δa_{tear} and Δa_{bl}; (b) presentation of the method for determining the unloaded CTOD δ^*_c.

CORRECTION FOR UNLOADING

The method described in the last section allows measurement of the unloaded value of the CTOD at cracking initiation, i.e. the opening of a blunted crack tip precisely before the first increment of ductile tearing. The parameter characterizing the resistance of the material to cracking initiation is the CTOD when the specimen is under loading. It is thus important to have a means for evaluating the CTOD before unloading, or, at least, a means for guaranteeing that the correction to be made to the unloaded CTOD is negligible. We insist on that, the focus here is only on the unloading of a static, blunted crack tip before any ductile tearing, i.e. the value of the CTOD obtained by the extrapolation on δ_1 - δ_2, and not on the effect of the unloading on a crack tip existing during crack propagation (as in Ref. [9]). Unloading can be analyzed in the following way [8]. The unloaded state is equivalent to the superposition of the two situations depicted in Fig. 2(a) and 2(b):

- the first situation is the specimen subjected to a tensile load *P* (Fig. 2a);
- the second situation is a specimen with an initially blunted crack tip subjected to a compressive load -*P* (Fig. 2b);
- the unloaded state corresponds to the superposition of (a) and (b). Fig. 2c shows the resulting stress field. A reverse plastic zone surrounded by the plastic zone due to the original loading thus develops, even for incomplete unloading of the specimen.

Based on the assumptions (i) of a perfectly-plastic behavior with similar yield stress in tension and compression (no Bauschinger effects, i.e. no difference between the behavior in tension and compression is assumed), but with a flow stress $\sigma_f = (\sigma_y + \sigma_u)/2$ in order to approximately account for some degree of strain hardening; (ii) of proportional plastic flow (which was already required for invoking the superposition of situations (a) and (b)); (iii) that the initial crack rounding of Fig. 2b is neglected; it will be shown that an estimate of the correction δ_{rev} to be applied to δ^*_c can be obtained, such that δ_c is given by

$$\delta_c = \delta^*_c + \delta_{rev} \quad (1)$$

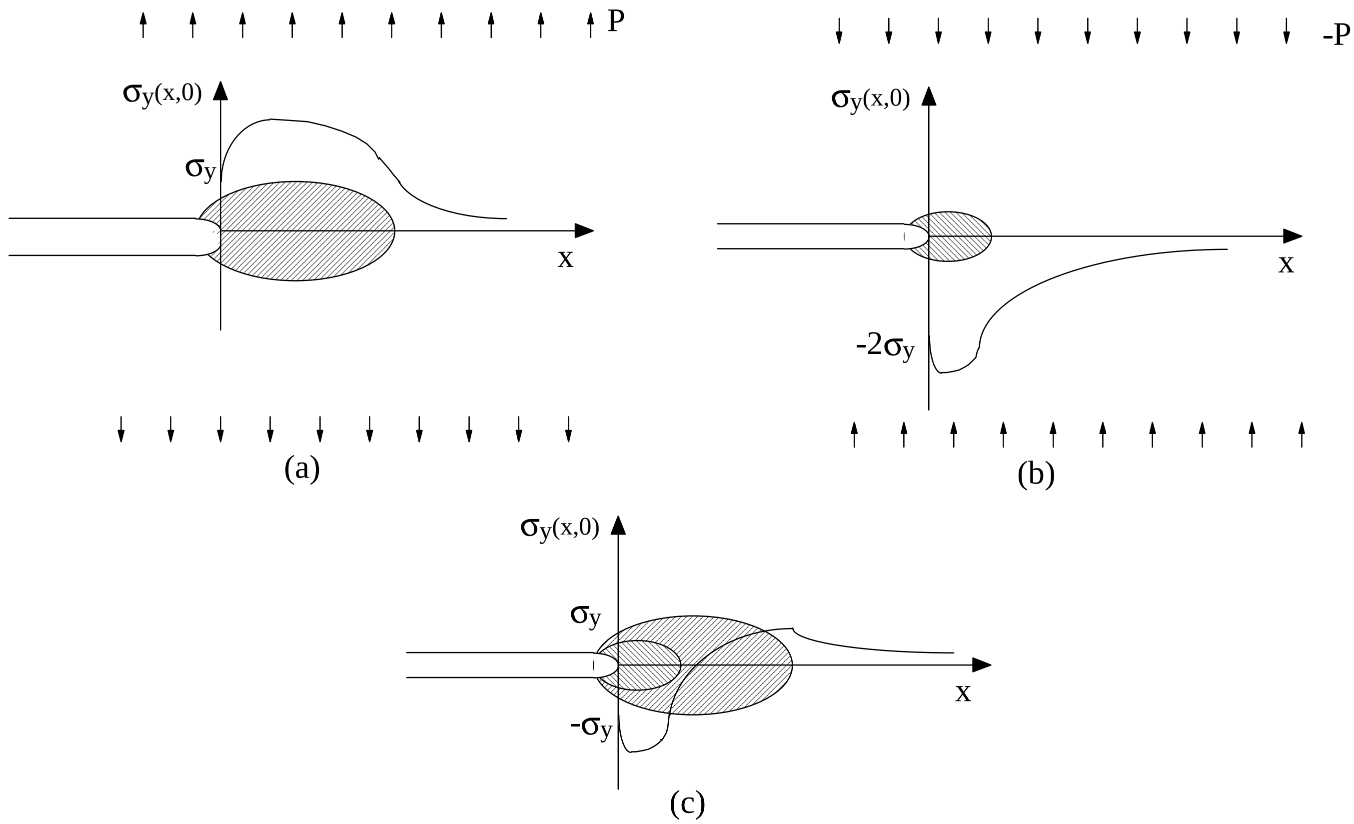

Figure 2. The superposition of (a) the stresses generated by a load *P* on a cracked specimen with a yield stress σ_y and (b) the stresses generated by a load -*P* on a cracked specimen with a yield stress in compression -2σ_y, gives (c) the unloaded solution.

Because of the assumed proportional loading and because no account is taken of the initial rounding of the crack, the effect of unloading is to reverse the direction of stresses in the reversed flow region. The changes in stresses, strains, and displacements due to load reduction are thus given by a solution identical to that for the original loading, but with the loading parameter replaced by the load reduction and the yield strain and stress replaced by twice their values for original loading [8]. In other words, any point which undergoes reversed yield will have experienced a change in stress from +σ_y to -σ_y and the superposition of the changes calculated with a yield stress 2σ_y (or 2σ_f to account for some degree of strain hardening) exactly represents the behavior. Unloading is equivalent to imposing, in compression, a stress intensity factor equal to K_c, where K_c is the stress intensity factor at cracking initiation during the original loading. The relationship between the energy release rate, *G*, and *K*, is

$$G = \frac{K^2\left(1 - \nu^2\right)}{E} \quad \text{(plane strain)} \tag{2}$$

The CTOD is related to J by the well-known relationship

$$\delta = d_n \frac{J}{\sigma_y} \quad , \tag{3}$$

where d_n has been tabulated by Shih [11]. Assuming small-scale reverse plasticity during unloading, *J* for the unloading is thus equal to -G_c, resulting in

$$\delta_{rev} = d_n \frac{J_c}{2\sigma_f} = d_n \frac{G_c}{2\sigma_f} = d_n \frac{K_c^2\left(1-\nu^2\right)}{E2\sigma_f} \tag{4}$$

where, accordingly, the yield stress has been replaced by twice the approximate current yield stress in the plastic zone at the end of the original loading, $2\sigma_f$.

If cracking initiates under SSY conditions during the original loading (and thus that $J_c^{loading} = J_c^{unloading}$), comparison of Eq. (3) and (4) shows that the unloaded CTOD will be half the loaded CTOD in perfectly plastic materials (i.e. with $\sigma_f = \sigma_y$). In other words, if the method presented in the last section is used on specimens presenting SSY at cracking initiation and low strain-hardening exponents, the correction given by Eq. (4) will be significant. Conversely, in fully yielded specimens, the correction may be tiny because the elastic part of J, J^{el} (= G) may be sometimes far smaller than the plastic part J^{pl}. Consequently, the relative importance of the correction on δ^*_c depends on the extension of yielding when cracking initiates. Comparison of Eq. (3) and (4) also shows that hardening decreases the relative importance of the correction to be applied to δ^*_c. It is worth noting that significant Bauschinger effect combined to SSY during loading and low strain hardening could bring about a correction for the unloading of the blunted crack tip larger than half the loaded CTOD.

The use of Eq. (4) as such relies on SSY conditions during reverse yielding. If the extension of reverse plasticity during unloading does not satisfies SSY, the use, in equation (4), of J_c^{el} (= G_c) will lead to an underestimation of the correction. Actually, the total J for unloading is required. The possibility for large-scale reverse yielding in small specimens of very ductile materials is real as it will be shown in the application of the next section. Many approaches have been proposed in the literature to evaluate the departure from SSY conditions (see for instance Hutchinson [12] Anderson [13]). One very simple, but limited, way to extend SSY concepts is Irwin's method [14] which requires the use of an effective crack length located in the center of the reverse plastic zone. The reverse plastic zone size r_{prev} is given by

$$r_{prev} = \frac{1}{3\pi}\left(\frac{K}{2\sigma_f}\right)^2 \tag{5}$$

where, again, the yield stress has been replaced by twice the approximate current yield stress in the plastic zone at the end of the original loading, $2\sigma_f$. Using the effective crack length an adjusted K can be computed (requiring a few iterations) and which can be used in (4).

In order to apply relation (4) for the correction of the experimental values of δ^*_c, K at cracking initiation, K_c, must be known. As the method presented in the last section is devoted to determine cracking initiation, K_c is thus not known. However, it is possible to approximately estimate the load at cracking initiation (and thus K) after having applied the method for determining δ_1 - δ_2. Indeed, the load P at which each specimen was unloaded can be plotted as a function of the crack advance Δa_{tear} and an approximate value of P at cracking initiation can be extrapolated to estimate K_c. This extrapolation brings about an error on the correction factor to be applied on δ_{rev}. Usually, for moderately to very LSY conditions, the load does not vary much after the onset of cracking, meaning that the error on the extrapolated value of K_c will be small.

The accuracy of Eq. (4) (accounting or not for possible non small-scale reverse yielding) can only be assessed by comparison with more accurate numerical calculations. Large strain finite element simulations were performed in Ref. [7] and proved that (4) is accurate for low to moderate strain hardening.

APPLICATION TO THE CHARACTERIZATION OF THE CRACKING INITIATION TOUGHNESS OF COPPER

The method described in the previous section has been adopted to evaluate the CTOD at cracking initiation of precracked Single Edge Notched Bend (SENB) specimens and Circumferentially Cracked Round Bars (CRB) made of cold-drawn copper [10]. Precracking of the SENB specimens was made using a resonance machine and the specimen were side-grooved (20% of the thickness). A rotative fatigue bending method was employed for precracking of the CRB specimens [10,15]. The a/W ratio of each specimens was always close to 0.5 (where a is the crack length and W the specimen width). Table 1 presents the main mechanical characteristics of copper. The Hollomon representation has been used:

$$\sigma = K\varepsilon^n \tag{6}$$

where n is the strain hardening exponent and K is a constant. Due to the succession of different hardening stages in copper, n varies with strain [16]. The value of n in Table I is thus an average value.

Fig. 3 shows a typical crack tip profile obtained on copper (for a small crack extension). Fig. 4 compares the variations of δ_1 - δ_2 as a function of Δa_{tear} for the two types of specimens, SENB and CRB. Each specimen was polished 6 times. Table 2 presents the extrapolated values of δ^*_c obtained using a linear regression.

TABLE 1

MAIN MECHANICAL CHARACTERISTICS OF COPPER: YOUNG'S MODULUS, E;
THE POISSON RATIO, ν; YIELD STRESS, σ_y; STRAIN AT NECKING, ε_u; STRESS AT NECKING, σ_u;
STRAIN-HARDENING EXPONENT IN A HOLLOMON POWER LAW REPRESENTATION, n; SHIH FACTOR, d_n.

Material	E (GPa)	ν	σ_y (MPa)	ε_u	σ_u (MPa)	n	d_n
Copper	121	0.35	312	0.008	325	≈0.1	0.7 (pl. strain)

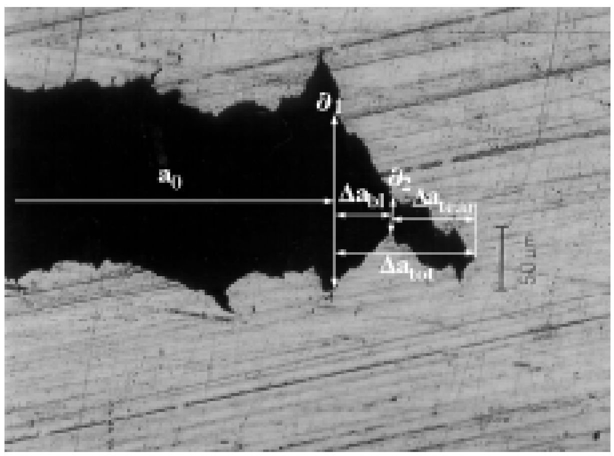

Figure 3. Micrograph of a typical crack tip zone corresponding to a small crack advance in a SENB copper specimen.

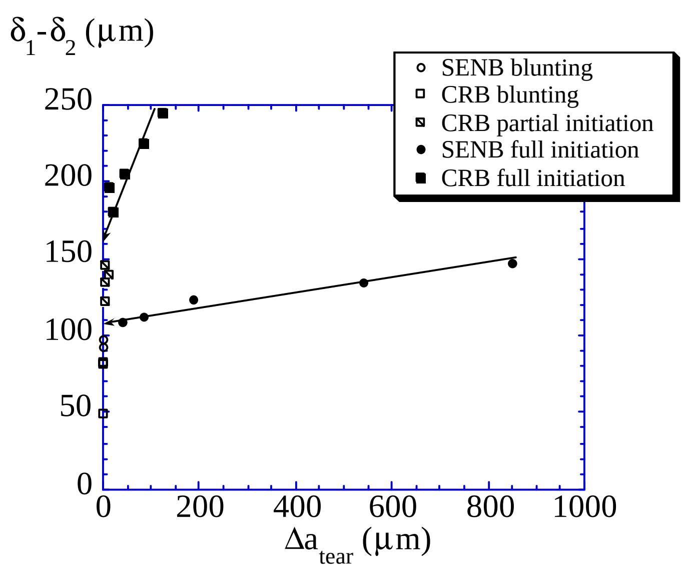

Figure 4. Variation of δ_1 - δ_2 as a function of the crack advance Δa_{tear}

for the SENB and CRB copper specimens.

TABLE 2

CRACK TIP OPENING PARAMETERS: UNLOADED CTOD AT CRACKING INITIATION, δ^*_c; CRACK CLOSING DUE TO REVERSE PLASTICITY, δ_{rev}; CTOD AT CRACKING INITIATION, δ_c; ENGINEERING CRITICAL CTOD, $\delta_{0.2}$.

Specimen type	δ^*_c (μm)	δ_{rev} (μm)	δ_{rev} improved using Irwin's method (μm)	δ_c (μm)	$\delta_{0.2}$ (μm)
SENB	106	6.8	7.8	114	185
CRB	160	8.4	10.1	170	

The closing of the crack caused by reverse plasticity during unloading, δ_{rev}, has been calculated using (4) and the best estimate of the load at initiation. The values of δ_{rev}, given in Table 2, are small with respect to δ^*_c. Indeed, cracking initiates while LSY conditions prevail in both specimens.[2] The reverse plastic zone sizes have been evaluated from (5): r_{prev} = 200 μm and 275 μm in the SENB and CRB specimens, respectively. The initial ligament lengths are equal to 3.5 mm and 2.5 mm in the SENB and CRB specimens, respectively. Both specimens thus involve large-scale reverse yielding during unloading. Use has been made of Irwin's model to infer a more precise value of δ_{rev}. Table II also presents the improved δ_{rev}. In [7], it has been shown that, with this final improvement, the analytical δ_{rev} agrees closely with the more exact δ_{rev} predicted by finite element simulation. However, Table 2 also proves that this correction is of little importance with respect to the total CTOD and could thus be omitted. The final δ_c are given in Table 2.

The fracture toughness at cracking initiation given by δ_c (or by the J_{Ic} which can be inferred from (3)) is significantly lower with the SENB specimens. Geometry effects on cracking initiation toughness are rarely mentioned in the literature. Typically, geometry effects are mainly observed during crack propagation (e.g. Joyce and Link [17]), caused by a loss of constraint (in [17] short crack or short ligament length effects). Here, the geometry effect is explained as resulting from a finite strain effect: the CRB specimen exhibits, at the same applied J, a finite strain zone 50% smaller than in the SENB specimen (see Ref. [10] for details). In the CRB geometry, a 50% larger applied J is thus required in order for a small representative element in the fracture process zone to reach the critical strain for void coalescence. In other words, J_{Ic} at physical cracking initiation is not a truly "intrinsic" material parameter in this case. The connection between J_{Ic} and the work spent per unit area in the fracture process zone depends on the loading configuration for the material of this study.

Finally, engineering value of the fracture toughness, $J_{0.2}$ (which consists in the intersection of the J_R curve with the 0.2 mm offset line parallel to the blunting line) have been measured for the SENB specimen in Ref. [10]. The engineering CTOD $\delta_{0.2}$ has been derived using (3). The value for $\delta_{0.2}$ is given in Table II. The significant difference between δ_c and $\delta_{0.2}$ demonstrates the interest of a robust method for predicting cracking initiation when accurate values of the physical fracture toughness are demanded.

CONCLUSIONS

The method proposed in this paper for the measurement of the CTOD at cracking initiation can be summarized as follows:

- A few precracked specimens are loaded in order to get crack extensions varying within the 0.05 mm to 1-2 mm range. The method requires a range of stable tearing in order to generate such crack advances.
- After unloading, the crack tip is observed at different locations along the crack front, by repetitive grinding and polishing. Three lengths are measured: δ_1, δ_2, and Δa_{tear} (see Fig. 1). For specimens presenting crack tunneling, it is important to perform measurements at the surface and at the center in order to get a good estimation of the average crack advance.

[2] The elastic and plastic parts of J can be compared in order to estimate the departure from SSY during the initial loading: J^{el} is roughly ten times smaller than J^{pl} in both CRB and SENB specimens.

- The value of δ_1 - δ_2 extrapolated for $\Delta a_{tear} \rightarrow 0$ is the unloaded CTOD at cracking initiation, δ^*_c. A linear regression was found adequate in the various cases addressed until now (see Ref. [7,10]).

Equation (4) can be used in order to evaluate the partial crack closing during unloading and determine the true CTOD at cracking initiation under load. The applied correction is significant when SSY or close to SSY situations prevail during original loading until cracking initiation. LSY during loading and large strain-hardening exponents decrease the importance of the correction. Bauschinger effects, low strain hardening, or LSY during unloading increase the relative importance of the correction.

ACKNOWLEDGEMENTS

The work of T. Pardoen was supported by a fellowship from F.N.R.S., Belgium, and by a grant from the B.A.E.F. Inc. Suggestions by Professor J. W. Hutchinson (Harvard University) about the reverse plasticity problem, and the contribution of M. Scibetta and R. Chaouadi (SCKCEN, Mol, Belgium) for the precracking of the specimens are gratefully acknowledged.

REFERENCES

1. ASTM Standard (1996). E1737-96, Standard Test Method J-Integral Characterization of Fracture Toughness. In *Annual Book of ASTM Standards*, Section 3, Volume 03.01, American Society for Testing and Materials, Philadelphia.
2. ESIS (1992). *ESIS Procedure for Determining the Fracture Behaviour of Materials*. European Structural Integrity Society.
3. Tvergaard, V. and Hutchinson, J.W. (1992). *J. Mech. Phys. Solids* **40**, 1377.
4. Li, D.M. and Bakker, A. (1997). *Engng. Fract. Mech.* **57**, 1.
5. Pluvinage, G. and Lanvin, A. (1996). *Fatigue Fract. Engng. Mater. Struct.* **16**, 955.
6. Ebrahimi, F. and Seo, H.K. (1996). *Acta Mater.* **44**, 831.
7. Pardoen, T. and Delannay, F. (2000). *Engng. Fract. Mech.* in press.
8. Rice, J.R. (1967). In *Fatigue Crack Propagation*, ASTM STP 415, American Society for Testing and Materials, 247-311.
9. Budiansky, B. and Hutchinson, J.W. (1978). *J. Appl. Mech.* **45**, 267.
10. Pardoen, T., Scibetta, M., Chaouadi, R. and Delannay, F. (1999). *Int. J. Fract.*, in press.
11. Shih, C.F. (1983). *Tables of Hutchinson-Rice-Rosengren Singular Field Quantities*, MRL E-147, Division of Engineering, Brown University, Providence, R.I.
12. Hutchinson, J.W. (1979). *Nonlinear Fracture Mechanics*, Department of Solids Mechanics, The Technical University of Denmark.
13. Anderson, T.L., *Fracture Mechanics – Fundamentals and Applications*, CRC Press, Boca Raton, 1995.
14. Irwin, G.R. (1960). In *Proceedings of the Seventh Sagamore Ordinance Materials Conference*, Syracuse University, IV.63-IV.78.
15. Scibetta, M. and Chaouadi, R. (1997). In *Small Specimen Test Techniques*, *ASTM STP 1329*, W. R. Corwin, S. T. Rosinski and E. van Walle (Eds.). American Society for Testing and Materials, Philadelphia.
16. Pardoen, T. and Delannay, F. (1998). *Metall. Mater. Trans. A* **29A**, 1895.
17. Joyce, J.A. and Link, R.E (1995). In *Fracture Mechanics: 26th Volume*, ASTM STP 1256, American Society for Testing and Materials, 142-177.